Research Square

Preprints are preliminary reports that have not undergone peer review.
They should not be considered conclusive, used to inform clinical practice,
or referenced by the media as validated information.

A Comparative Analysis of Nyquist versus 3GPP Sampling Rates in Advanced Multi-rate Systems

Zakka Augustine

zax.austen@yahoo.com

University of Hralove Kralove https://orcid.org/0000-0002-7366-7071

Research Article

Keywords: 3GPP sampling standard, Nyquist sampling method, Multi-rate information frameworks, Bandwidth utilization, Data communications

Posted Date: November 16th, 2026

DOI: https://doi.org/10.21203/rs.3.rs-11721679/v1

License: This work is licensed under a Creative Commons Attribution 4.0 International License.
Read Full License

Additional Declarations: The authors declare no competing interests.

A Comparative Analysis of Nyquist versus 3GPP Sampling Rates in Advanced Multi-rate Systems

Zakka Augustine [a], Gideon Nuhu [a], Yayock Amos Takai[b], Franklin Chibueze Njoku[c], Stella Ngozi Obiahu[d]

[a] Department of Computer Sciences, Faculty of Computing, Federal University of Applied Sciences, KM 100 Kachia/Kafanchan Rd, Kachia, Nigeria.
[b] Department of Information Technology, Faculty of Computing, Federal University of Applied Sciences, KM 100 Kachia/Kafanchan Rd, Kachia, Nigeria
[c] Department of Telecommunications Engineering, Faculty of Ground Engineering, Air Force Institute of Technology, Kaduna 800282, Nigeria.
[d] Department of Control Engineering, Faculty of Engineering, Ahmadu Bello University, Zaria, Nigeria.
Corresponding Author Email: zax.austen@yahoo.com,

Abstract
Continuous analogue signals in wireless systems require constant sampling to manage information transmission burdens, yet these signals are prone to degradation and distortion due to inefficiency in bandwidth utilization. In wireless communications, like Long Term Evolution (LTE) and 5th Generation (5G) New Radio (NR), strict adherence to the standard Nyquist-Shannon sampling theorem encounters major hardware and computational bottlenecks. To mitigate these challenges, this research presented a computational analysis between Nyquist and 3rd Generation Partnership Project (3GPP) sampling methods at varying frequencies. The results obtained recorded that the 3GPP standard is more sufficient for modern data analysis requirement than the Nyquist method, wasting only 25% of bandwidth compared to 50% of Nyquist. Considering experimental results at 960 Guard Interval (GI) of 400 MHz, the 3GPP method perfectly aligns by obtaining 960 kHz tone-space, while the Nyquist misaligns with an increase overhead of 993.6 kHz due to arbitrary clock grid. This dramatic clock-rate reduction directly translates into tangible hardware benefits, including lower power consumption, higher bit-resolution, and reduced implementation costs. While Nyquist is proven suitable for 4G LTE and earlier versions of air-interface systems, the 3GPP standard offered superior bandwidth utilization, making it better for 5G NR and 6G data deployments.

Keywords: 3GPP sampling standard, Nyquist sampling method, Multi-rate information frameworks, Bandwidth utilization, Data communications.

Introduction

Converting continuous analogue data streams to digital data requires three core steps: sampling (capturing discrete time intervals), quantizing (rounding values to discrete levels), and encoding (assigning binary codes) [1]. Sampling is a process of separating desired signals from a mixture of undesired signals [2], [3]. In wireless data transmission, physical waves degrade during transmission [4], [5]. Optimizing these processes on baseband signals is vital for maximizing spectrum capacity to meet the demands for modern 5th Generation (5G) and 6th Generation (6G) networks [6], [7]. This is because the rapid proliferation of mobile broadband and the continuous evolution toward 6G ecosystems demand highly efficient data transfer mechanisms [8], [9]. The foundation of these wireless architectures lies in the management of continuous analog information signals [10], [11]. To manage information transmission burdens and make these signals compatible with modern digital systems, constant sampling is required [12]. However, raw analog data signals are inherently prone to distortion, including interference, noise, and scattering that causes degradation during this conversion process [13]. Therefore, selecting an optimal sampling methodology is vital for maintaining high signal integrity without wasting channel bandwidth [14].

Traditionally, the Nyquist-Shannon theorem has served as the baseline for analog-to-digital signal conversion [15]. While the Nyquist methodology provides a reliable framework for older generations of mobile broadband, particularly 4th Generation (4G) LTE-Advanced (LTE-A) networks, its rigid sampling rates often result in excessive overhead [16]. Comparative analyses of sampling methods reveal that Nyquist-based data sampling can waste up to 50% of available transmission bandwidth. In

contrast, the 3rd Generation Partnership Project (3GPP) has established standardized sampling techniques that offer a marked improvement in efficiency [17], [18]. This study demonstrates that the 3GPP standard limits bandwidth waste, effectively recovering a significant portion of the spectrum for active data transmission [19], [20].

Furthermore, as global networks shift toward dense deployments and ultra-wideband scenarios, spectral efficiency remains a primary Key Performance Indicator (KPI) [21], [22]. While Nyquist data sampling is completely suitable for standard 4G networks and earlier generations, its bandwidth waste becomes a major bottleneck for the high-data-rate (throughput), high-capacity demands of 5G NR, and forthcoming 6G architectures [23], [24]**.** The 3GPP standard offers vastly superior bandwidth utilization, rendering it significantly better suited for the complex modulation schemes, broader frequency ranges, and massive Multiple-Input Multiple-Output (MIMO) configurations required by these advanced networks [25], [26], [27].

This study aims at investigating the performance metrics of baseband data signal sampling methods, with a primary focus on quantifying the transmission efficacy between traditional Nyquist methods and 3GPP standards in modern systems. By evaluating bandwidth utilization, signal degradation risks, and overall transmission efficiency, this research will demonstrate how 3GPP standard alleviates data bottlenecks like, hardware cost, system power consumption, real-world transition, bandwidth utilization, effective orthogonality, and clock synchronization constraints to meet the rigorous demands of emerging 5G NR and 6G network deployments. From this stated background, the following research objectives are conceived and addressed:

- To evaluate and quantify the transmission efficacy and overall system efficiency of traditional Nyquist sampling methods versus 3GPP standards in modern wireless systems.
- To analyze how 3GPP oversampling and digital guard bands manage non-ideal analog filter transition bands and prevent signal aliasing.
- To assess how 3GPP Complex Quadrature (I/Q) sampling lowers the sampling rate per Analog-to-Digital Converter (ADC) path, reducing high hardware expenses, low bit-resolution, and excessive power consumption.
- To investigate how linking 3GPP sampling rates to Subcarrier Spacing (SCS) and Fast Fourier Transform (FFT) sizes mitigates Inter-Symbol Interference (ISI) and Inter-Carrier Interference (ICI) using advanced air interface architectures.
- To demonstrate how 3GPP standardizations overcome real-world transition, clock synchronization, and bandwidth bottlenecks to meet the demands of emerging 5G NR and 6G networks.

Significance of Study

The core bottleneck of the rigid, theoretical Nyquist sampling rate that the 3GPP standards need to solve are the difficulties experienced in the implementation of ideal mathematical filters and strict hardware boundaries in real-world wireless systems. Specifically, this research is engineered towards overcoming three interlinked physical bottlenecks experienced by Nyquist using 3GPP sampling method. These are:

- **The Real-World Filter Transition Band Bottleneck:** The Nyquist theorem assumes the use of an ideal, theoretical brick-wall low-pass filter to perfectly reconstruct a signal. Consequently, ideal filters are known to have a transition band of zero Hz, which cuts off instantly. Native ADCs and Digital-to-Analog Converters (DACs) use casual, non-ideal analog filters. As such, they require a gradual "transition band" to roll off energy smoothly from the edge of the channel to absolute silence. The 3GPP method is required to proffer a solution to this pitfall to prevent aliasing in this non-ideal transition zone using 3GPP oversampling combined with digital guard bands.

- **High Hardware Costs and Power Consumption:** As wireless bands expand into millimeter wave (mmWave) of 5G/6G and reach gigahertz widths, the Nyquist method runs into major issues, strictly scaling ADCs to match twice the maximum frequency, which severely pushes hardware to its absolute limits. Ultra-high-speed ADCs are expensive, suffer from reduced bit-resolution, and drain enormous amounts of battery power. The 3GPP is expected to address this by standardizing I/Q sampling. By splitting the received Radio Frequency (RF) signal into In-phase, *I, and* Quadrature, Q, components via a local oscillator, the bandwidth is split evenly between the positive and negative spectrum. Because the I and Q paths are processed independently, the required sampling rate per ADC path drops down to exactly match the bandwidth, instead of twice the highest frequency.
- **The Orthogonality and Clock Synchronization Constraint:** The Nyquist sampling cares only about reconstructing a continuous waveform. It does not account for the strict phase and timing relationships needed to keep thousands of overlapping orthogonal subcarriers (for example, the Orthogonal Frequency Division Multiplexing (OFDM) framework) from bleeding into one another. The 3GPP dictates that the system sampling rate must be a strict mathematical derivative of the Subcarrier Spacing (SCS) and the FFT size. In this light, linking the sampling rate directly to a power-of-two FFT matrix, the 3GPP technique will guarantee sampling intervals that align flawlessly with the Cyclic Prefix (CP) and symbol boundaries. This completely solves Inter-Symbol Interference (ISI) and Inter-Carrier Interference (ICI) bottlenecks that Nyquist theory ignores.

Review of Similar Work

In view of the need for advanced information sampling techniques that could improve bandwidth utilization, there is a need to review prior research that has made notable and constructive improvements to the traditional Nyquist sampling scheme. This work builds on these earlier methods to effectively demonstrate the effectiveness of this research when deployed at higher frequencies.

In order to mitigate computational complexity and hardwire bottlenecks experienced in the traditional Nyquist-Shannon sampling method, [28] proposed a single-channel, frequency-shifting sub-Nyquist framework with Adaptive Residual Energy Detection (ARED). This is to simplify wideband spectrum sensing by eliminating the need for prior knowledge of spectrum sparsity. While simulation results indicate performance comparable to or exceeding that of traditional Modulated Wideband Converters (MWC) by overcoming hardware sampling bottlenecks encountered in LTE and earlier air interface systems, the approach faces increasing sensing-time constraints and requires validation against physical hardware imperfections. [29] proposes a low-sampling-rate receiver for 6G multi-antenna multi-user OFDM systems, reducing the Analog-to-Digital Converter (ADC) sampling rate to (1/K) of the Nyquist rate, thereby reducing energy consumption and hardware costs. By employing Zero-Forcing (ZF) precoding, the design maintains negligible performance degradation in bit error rate and peak-to-average power ratio, although it increases transmitter complexity and relies heavily on precise Channel State Information (CSI). [30] introduced a novel sub-Nyquist Photoacoustic Computed Tomography (PACT) imaging method that enables high-frequency imaging, achieving a 22 μm axial resolution with a 30 MHz transducer and 41.67 MHz sampling rate. While this approach offers high-resolution, cost-effective imaging validated through simulations and experiments, it is better suited to biological imaging applications than to conventional communication. The signal-processing principles are relevant to 5G/6G advancements. [31] demonstrates that a 28 GHz, 2.52 GHz IF sub-sampling receiver achieves significant power reduction in 5G mm-wave systems by utilizing lower Analogue to Digital Conversion (ADC) sampling rates. While relying on aliasing introduces susceptibility to noise, the approach is highly viable, incurring only a 3 dB SNR penalty at a 5% BLER for QPSK signals, making it an efficient alternative to direct RF sampling. However, the method requires careful consideration of

the trade-offs between reduced receiver hardware and signal-quality metrics such as EVM and Block Error Rate (BLER). [32] presented a sub-Nyquist sampling rate temporal correlation method to eliminate parasitic reflections during the measurement of transparent planar elements, achieving high-accuracy front surface reconstruction with a 113 nm RMS error. By analyzing temporal intensity sequences and reducing the required fringe patterns to fewer than 500, the approach significantly reduces computation time to 205 seconds, compared to 1000 seconds for conventional methods. While offering improved efficiency, the method focuses primarily on front-surface reconstruction without addressing the simultaneous decoupling of the back surface. [33] proposed the Faster-Than-Nyquist Generalized Frequency Division Multiplexing Access (FTN-GFDMA) scheme, which facilitates 6G rural connectivity for enhanced Remote Area Communication (eRAC) by utilizing sub-gigahertz and Television White Space (TVWS) frequencies and avoiding inter-user interference, offering improved spectral efficiency compared to traditional Nyquist methods. While the approach achieves higher user throughput and network capacity without compromising Bit Error Rate (BER), it increases detection complexity.

In view of these diverse attempts by existing work to address the limitations of conventional Nyquist sampling through different approaches. It is noted that the methods used experienced some constraints, including introducing signal processing delay, anomalies from physical hardware imperfections, signal overlapping, and reduction in signal quality on the receiver side. Considering these anomalies, this research presents an advanced approach based on the different tone-spaces proposed by 3GPP to improve data transmission fidelity in 5G NR and 6G systems.

System Modelling

The modelling in this research encompasses the materials and methods used to implement the research methodology. The section explains the foundational principles of sampling, as well as the tools for analyzing baseband samples for effective data transmission.

Baseband

Inasmuch as this is the fundamental signal to be transported, it can be called the base-signal, and the frequency band that contains it can be called the baseband. Transporting information signals in this frequency range can pose monumental difficulties; as such, there is a need to always transform this signal to a form that suits its carrier band [34,35]. In this light, this research runs a simulation to test the efficacy of the conventional Nyquist sampling in comparison to the proposed 3GPP sampling models in higher air-interface frequencies.

Oversampling

Oversampling is a data augmentation technique utilized to address class imbalance problems in which one class significantly outnumbers the others [36]. It aims to rebalance the training data distribution by increasing the number of instances from the under-represented class [37].

The Nyquist sampling rate is a theoretical limit, while the 3GPP sampling rate is a standardized, practical sampling frequency used in wireless communication networks such as 4G (LTE) and 5G (NR) to balance signal fidelity with hardware processing efficiency. The key differences between the two concepts lie in their purpose, value, and application.

Nyquist Sampling Rate (Theoretical Rule)

It is the minimum rate required to convert an analog signal into digital form without losing any information or causing "aliasing" (signal distortion). It ensures the perfect mathematical reconstruction of a continuous signal from discrete samples. It is better suited to theoretical signal processing concepts

than to hardware standards. Fig. 1 presents a generic workflow diagram of a simple Nyquist sampling model.

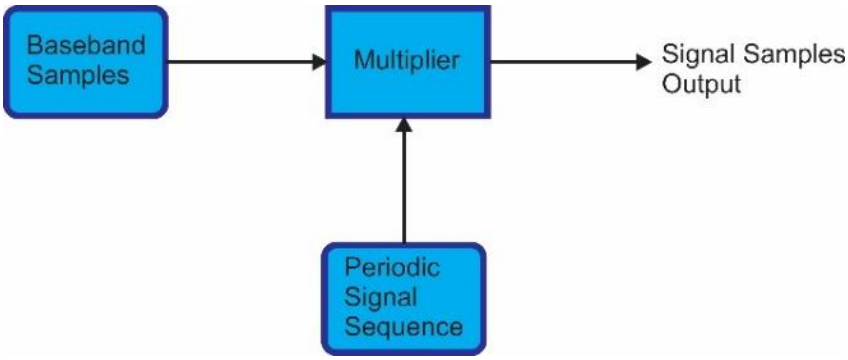


Fig. 1 Simple Nyquist Sampling Model

The conventional Nyquist theorem indicates that, for a proper reconstruction of a band-limited analog signal, the sampling frequency, f_S should be at least equal to twice the signal B, that is, the Nyquist rate f_{Nyq} of the signal [39].

$$f_S \geq f_{Nyq} = 2 \times B \tag{1}$$

where B is the highest frequency component or nominal bandwidth of the signal

3GPP Sampling Rate (The Practical Standard)

It is the standardized clock-and-sampling-frequency model defined by the 3GPP for baseband digital signal processing in mobile networks. Unlike the pure $2 \times B$ formula, 3GPP fixes its sampling rates to cleanly accommodate hardware capabilities (like Fast Fourier Transform (FFT) sizes). Its purpose is to manage resource grids, carrier spacing, and timing to prevent guard-band interference at the edges of the channel. It is a strictly enforced, highly engineered standard in cellular technology [38]. Fig. 2 presents a typical LTE transceiver model deployed by 3GPP sampling method, which is mostly realized using quadrature system analysis.

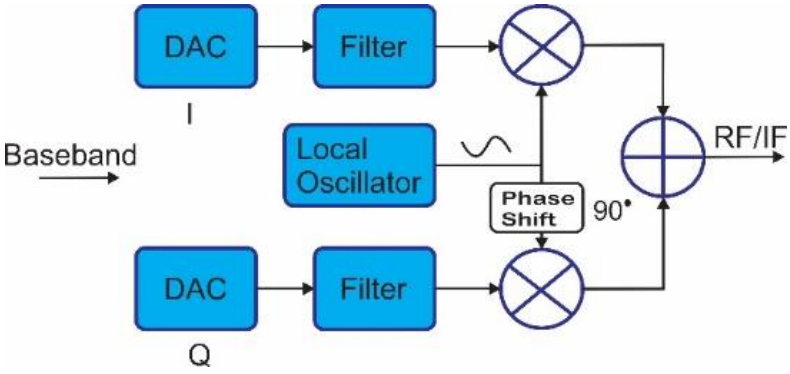


Fig. 2 Quadrature Transmitter System

Consequently, the 3GPP sampling frequency intentionally uses an oversampling technique, expressed as:

$$f_S = \frac{\Delta f_{max} . N_f}{m} \tag{2}$$

where:

f_S is the sampling rate.

N_f denotes the multi-rate (MR) symbol length or FFT size.

Δf_{max}stand for the subcarrier spacing,

m represents an integer that goes from 1 to N_f, which gives the index of each frequency point.

In conversed, the carrier sampling time is given as the inverse of f_S and is calculated here as:

$$T_C = \frac{1}{(\Delta fmax.Nf)} \quad (3)$$

where, T_C is the sampling time.

In view of the current high demand for bandwidth and reduced system complexity caused by hardware burdens, the 3GPP recommends deploying its sampling model for 5G NR and beyond 5G frequencies instead of using equation (1).

Transmission and Operational Bandwidth

Transmission bandwidth is the total frequency spectrum required to transmit a specific signal without distortion, measured in Hertz (Hz). Operational bandwidth is the assigned, usable channel width a system actively utilizes within a broader band, dictating the maximum data rate (throughput) measured in bits per second (bps). There is always a need to convert the baseband information to suit both the transmission frequency and the data rate. The proposed transmission bandwidth for each *N* number of subcarriers as considered in this work is expressed in equation (4) of [40] as follows:

$$\Delta_w = \frac{BW_{max}}{N} \quad (4)$$

where, *BW*max is the maximum channel bandwidth allotted for each air interface in compliance with the 3GPP specification, and *N* is the same as the total IFFT/FFT points.

The maximum number of bandwidths, or the total channel bandwidth of a conventional orthogonal multi-rate for 4G systems, is 20 MHz. This befits a 64 IFFT/FFT subcarrier size, an SCS of 15 kHz, and occupies a bandwidth of 16.6 MHz so far. A simple example is OFDM, with $2^6 = 64$subcarriers, which encompasses 52 useful subcarriers (that is, 48 effective data (payload) subcarriers and 4 pilot subcarriers), and 12 subcarriers as Guide Interval (GI). This is occupying a duration, *T* of 4.0 µs of useful symbols (that is, an effective data duration, *TS* of 3.8 μs and a CP duration of 0.2 μs). This total number of subcarriers per orthogonal symbol uses either 64 modulated APSK, QPSK, or 64-QAM constellations.

Results and Discussion

This section presents the results obtained in the simulations carried out in this work. The materials used for the realization of the results include PyCharm IDE 3.10.8 of Python, the 2048 FFF tool for system test-run, 8192 IFFT/FFT samples of length 1/16 convolutional tone space, 1080 control data (pilots), a 512QAM mapping scale of 9 bits each, an orthogonal multi-rate framework of OFDM and its upgraded variants, and 5G NR and 6G air-interface frequencies.

Sampling Frequency and Sampling Time Analysis

The conventional Nyquist theorem that derives the relationship between data signal frequency and bandwidth is obtained as in [41]. Therefore, for a 2048 FFT/IFFT size of an LTE multi-rate system, the Nyquist sampling rate at 20 MHz operational bandwidth is expressed in equation (1) as:

$$f_S = 2 \text{ x } 20 = 40 \text{ MHz} \quad (5)$$

Thus, the 3GPP sampling equation for 4G LTE tone space based on quadrature modulation, with a 15 kHz tone spacing, a 2048-point FFT/IFFT size, and m = 1 (since there is no indexing in this context), yields the sampling rate given by equation (2).

$$f_S = \frac{\mathbf{15{,}000\ x\ 2048}}{\mathbf{1}} = 30.72 \text{ MHz} \quad (6)$$

The 30.72 MHz rate obtained clearly aligns with standard mathematical transforms as:

- The tone space is mathematically set to 15 kHz.
- To effectively perform a power-of-2 FFT analysis, an FFT size of 2048 is used.
- Multiplying these two yields: 15 kHz×2048 = 30.72 MHz.
- Sample index, $m = 1$

While the Nyquist theorem of equation (5) states a 20 MHz channel, the baseband signal only needs to be sampled at 40 MHz (or 20 MHz if taking as complex, In-phase, and Quadrature (I/Q) samples). However, 3GPP sets the rate to 30.72 MHz for a 20 MHz channel, with 75% bandwidth utilization, compared to 50% achieved by Nyquist in equation (5). Fig. 3 presents simulation results of the real-world filter transition band pitfalls experienced in the Nyquist sampling method but mitigated by 3GPP.

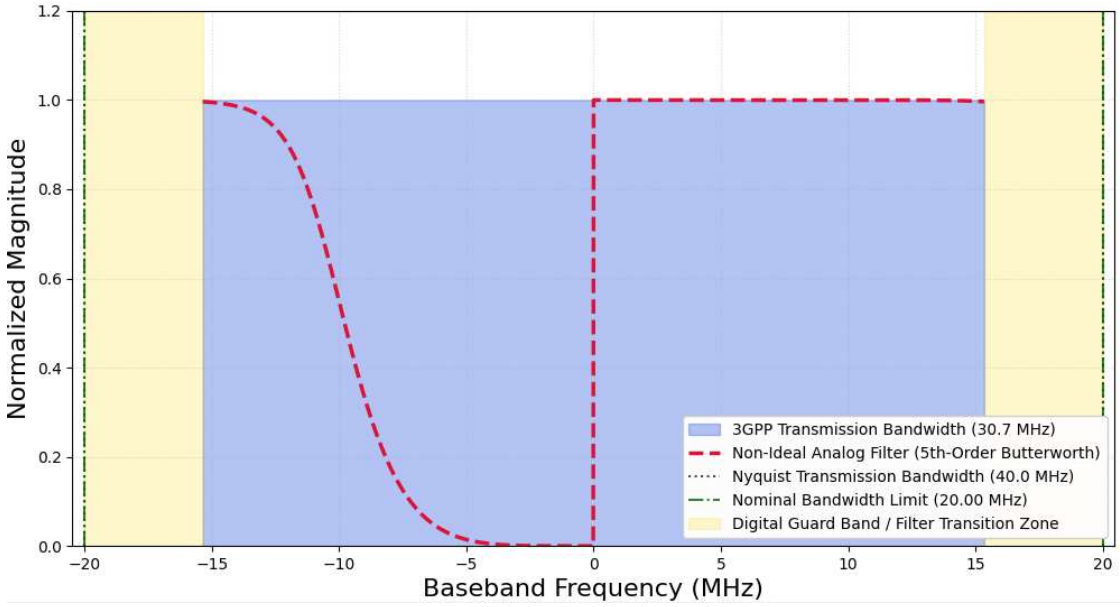


Fig. 3 3GPP vs. Nyquist Sampling Methods Solution to Real-World Filter Transition Band Bottlenecks at 20 MHZ LTE

It is worth noting that for an LTE baseband signal with a BW of 20 MHz, the minimum 3GPP sampling rate required to convert it to the digital domain is 30.72 MHz, as computed in equation (6). The number 30.72 MHz is also captured on the 3GPP LTE specifications, for example, in TS 36.101. This has raised so many questions regarding the Nyquist sampling theorem, which states that "sampling frequency should be at least twice that of the signal bandwidth." Instead of a 40 MHz round number for

a 20 MHz BW, 3GPP obtained 30.72 MHz. This discrepancy occurs when using a 'quadrature sampling system or module' and when adopting the OFDM-type of tone-space signal generation, as is the case in this work. Fig. 4 shows a simulation result of an LTE signal with a 20 MHz BW using quadrature modulation, which obtains a 10 MHz complex-signal bandwidth path. The system contains individual mixers that carry signals within certain bandwidths. When combined, they provide a total of 20 MHz bandwidth. Each of the paths with individual bandwidth has the baseband sampling rate of 30.72 MHz, which is three times (3x) the Nyquist sampling rate.

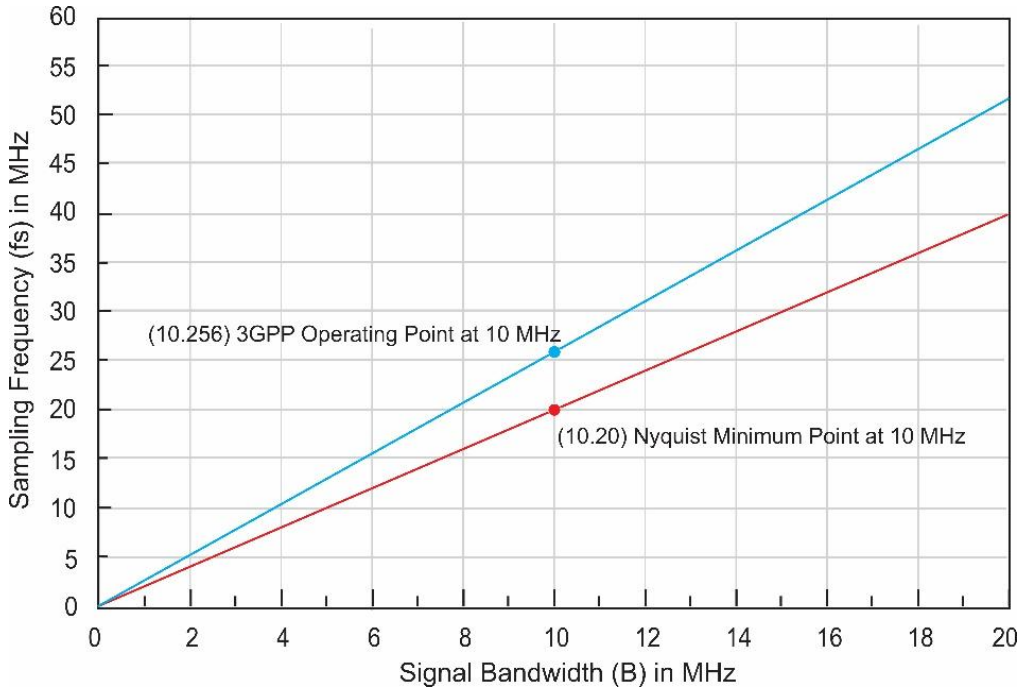
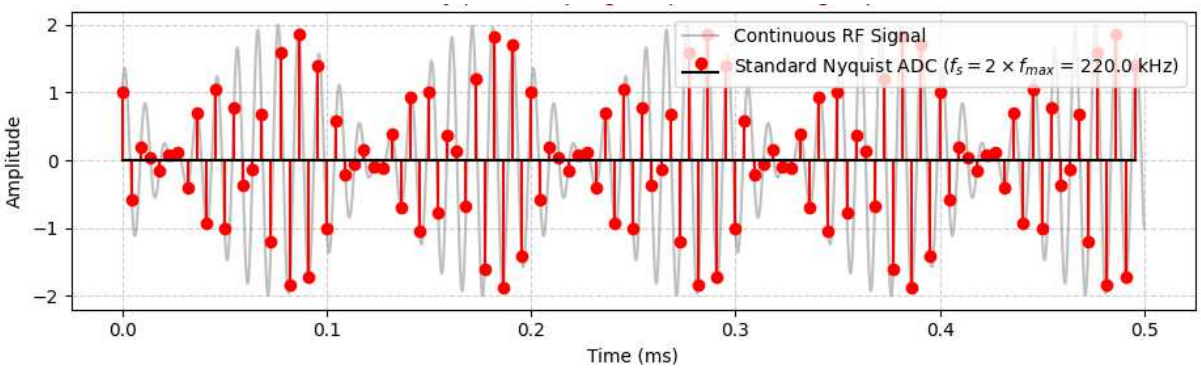
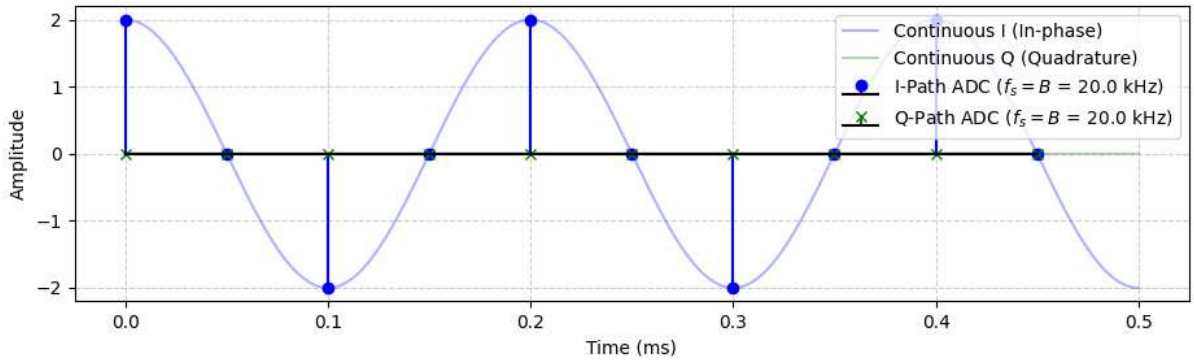


Fig. 4 System sampling Frequency: Nyquist vs. 3GPP Sampling Constraints

To compare the hardware impact on the wireless channel based on modern system expectations, simulations are conducted on the standard RF Nyquist sampling and the 3GPP complex quadrature I/Q sampling. In reality, mmWave operates in GHz, but it is scaled here to MHz/kHz in order to achieve clean plots. Figure 5 demonstrates the 3GPP solution to real-world hardware bottlenecks experienced by Nyquist method at 20 MHz LTE.



(a) Standard RF Nyquist Sampling



(b) 3GPP Complex Quadrature (I/Q) Sampling

Figure 5: ADC Sampling Rate Reduction: Nyquist vs 3GPP Complex Quadrature (I/Q) at 20 MHz.

The 3GPP-standardized digital GI length template/option that ensures effective data transmission is decomposed and illustrated in Table 1 [42]. This has informed the choice of the pilot data for this work.

Table 1 Subcarrier Samples Relative to GI length

Inputs		Subcarrier Sample **Options**								
		32	**64**	**128**	**256**	**512**	**1024**	**2048**	**4086**	**8192**
Standard GI Length	**¼**	8	16	32	64	128	256	512	1024	2048
	1/8	4	8	16	32	64	128	256	512	1024
	1/16	2	4	8	16	32	64	128	256	512
	1/32	1	2	4	8	16	32	64	128	256

Table 2 provides a detailed analysis of the various sampling times and sampling frequencies relative to their respective tone-spaces, sample sizes, bandwidths, and air interfaces. This work considers 2^{13} = 8192 subcarrier FFT as its peak points (consisting of 7680 effective data-carrying symbols, 1080 pilot data, and 512 GI slots), which are transmitted within a 400 MHz bandwidth. The 8192 data samples are used in all tone spaces in order to explore the effectiveness of the GI in achieving 4G, LTE-A, 5G FRI/FR2//FR-A, and 6G waveforms for the purpose of advanced transmission.

Table 2 3GPP Standard of T_C and f_S Relationship with SCS, N_f, and BW

Numerology (μ)	**Tone Space (kHz)**	**Sampling Time, T_C (ns)**	**Sampling Frequency, f_S (MHz)**	**IFFT/FFT Size (N_f)**	**Maximum Bandwidth (BW)**	**MC Channel Access**	**Air Interface**
0	15	2083.333	0.48	32	20 MHz	OFDM	4G LTE
1	30	520,833	1.92	64	50 MHz	CP-	LTE-
2	60	64.935	15.36	256	100 MHz	OFDM	A/FR1
3	120	8.136	122.88	1024	200 MHz	F-OFDM	5G FR1
4	240	?	?	2048	400 MHz	F-OFDM	FR1/FR2
5	480	?	?	4096	400 MHz	?	5G FR2
6	960	?	?	8192	400 - MHz	?	FR2-A

Table 3 demonstrates FF-OFDM's ability in sampling time, T_C and sampling frequency, f_S at 8192 subcarriers and sub-band bandwidth of m = 1.

To successfully obtain the required signal waveform data bits for interference estimation, the modulation scheme adopted in this work is QAM. For example, 16QAM is a QAM scheme with 16 symbols with 4 data bits (2^4 = 16), which obtains a 48 Mbps maximum data rate; 64QAM contains 64

symbols with 6 data bits (2^6 = 64), which achieves a 72 Mbps maximum data rate; and 256QAM contains 256 symbols with 8 data bits (2^8 = 256), achieving twice the data rate of 16QAM, which is 96 Mbps.

To align with the requirements of the present and next generations of the EU and adhere to the 3GPP specifications for 5G NR, this research adopted 512-QAM for its modulation process. This is intended to drive 9 bits per symbol of 8192 subcarriers. This would intentionally enable the effective transformation of data from the frequency domain to the time domain and vice versa. The 512-QAM is an adaptive modulation method that offers increased sensitivity, specificity, and accuracy for detecting useful baseband data.

Table 3 T_C and f_S Parameters for 8192 Subcarrier Samples Size at m = 1

IFFT/FFT Size (N)	Tone Space (kHz)	Sampling Frequency, f_S (MHz)	Sampling Time, T_C (ns)	Maximum Bandwidth (BW)	MC Channel Access Technique	Air Interface
8192	15	122.88	8.14	20 MHz	OFDM	4G LTE
8192	30	245.76	4.07	50 MHz	CP-OFDM	LTE-A/5G
8192	60	491.52	2.03	100 MHz	F-OFDM	5G FR1
8192	120	983.04	1.01	200 MHz	F-OFDM	FR1/FR2
8192	240	1966.08	0.51	400 MHz	FF-OFDM	FR2/FR2-2
8192	480	3932.16	0.26	400 MHz	FF-OFDM	FR2-2/A
8192	960	9864.32	0.23	400 MHz	AI-enabled	FR-A/6G

Tables 4 and 5 show what is obtainable from the 8192 subcarriers and sampling rate/time of various tone spaces, as enshrined by the 3GPP NR projection. These also display the sampling time, T_C and sampling frequency, f_S parameters computed/coded in this work for higher air interfaces. Sampling is performed on the baseband signal; as such, this research chose N_B = 7680 as the number of subcarriers constituting baseband information (pilots and payloads) and also considers K = 160 subbands, and m = M = 48 subcarriers (index sample) per subband bandwidth to show the scalability of the 3GPP model in handling high data samples. The more samples, the higher the sensitivity and accuracy in mitigating sampling anomalies in the system. While Table 4 shows the block sampling outcome per tone-space, at unity subband bandwidth, Table 5 also shows the overall sampling efficiency per each subband bandwidth, The results from the simulation are projected to fall within the 3GPP standard prospective waveforms.

Table 4 T_C and f_S Parameters for 7680 Baseband Data Samples Size at m = *1*

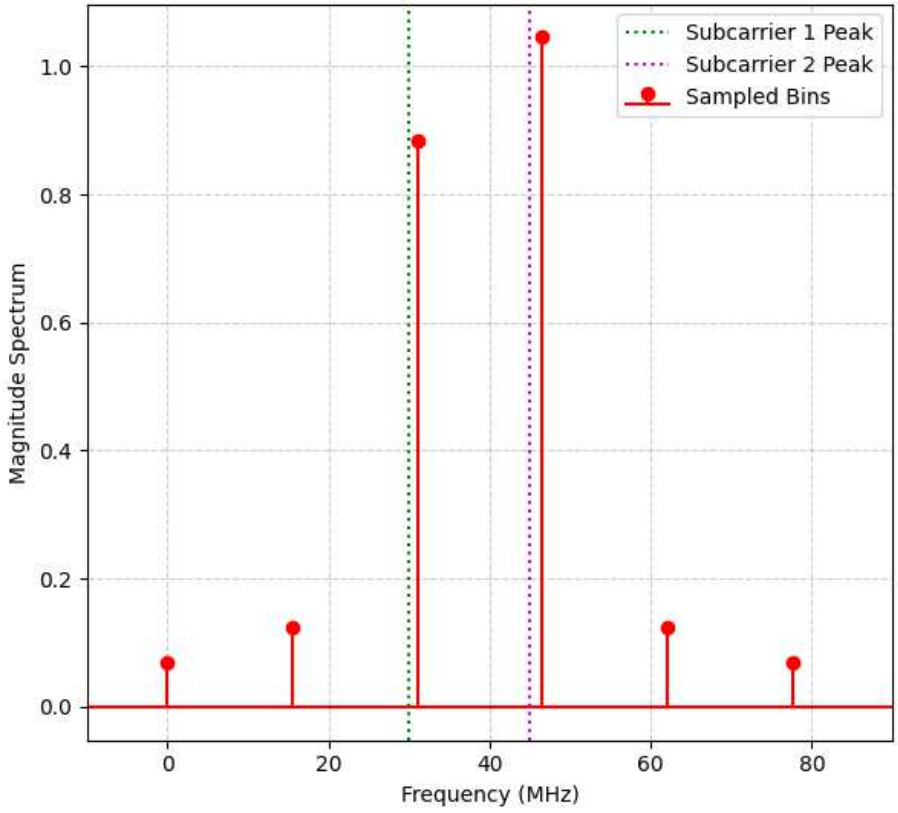
IFFT/FFT Size (N_B)	Tone Space (kHz)	Sampling Frequency, f_S (MHz)	Sampling Time, T_C (ns)	Maximum Bandwidth (BW)	MC Channel Access Technique	Air Interface
7680	15	115.2	8.68	20 MHz	F-OFDM	5G FR1
7680	30	230.4	4.34	50 MHz	F-OFDM	5G FR1
7680	60	460.8	2.17	100 MHz	F-OFDM	5G FR1
7680	120	921.6	1.08	200 MHz	FF-OFDM	FR1/FR2
7680	240	1,843.2	0.67	400 MHz	FF-OFDM	FR2/FR2-2
7680	480	3686.4	0.34	400 MHz	FF-OFDM	FR2-2/A
7680	960	7372.8	0.17	400 MHZ	AI-enabled	FR-A/6G

Table 5 T_C and f_S Parameters for 7680 Baseband Data Samples Size at m = M = 48

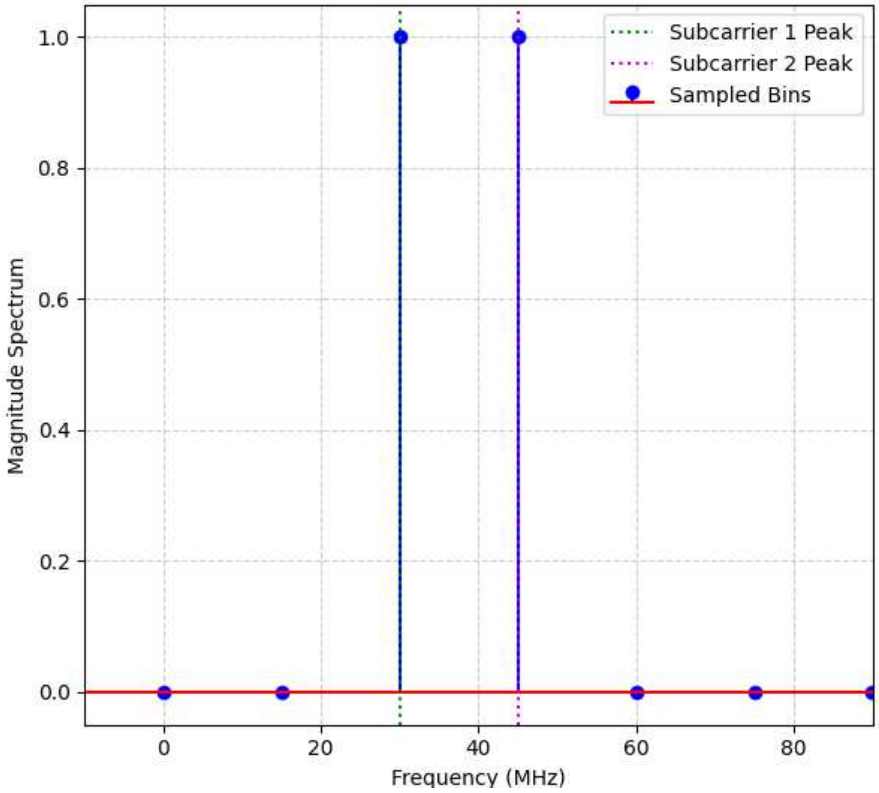
IFFT/FFT Size (N_B))	Tone Space (kHz)	Sampling Frequency, f_S (MHz)	Sampling Time, T_C (ns)	Maximum Bandwidth (BW)	MC Channel Access Technique	Air Interface

7680	15	1.2	466.66	20 MHz	F-OFDM	5G FR1
7680	30	2.4	208.33	50 MHz	F-OFDM	5G FR1
7680	60	4.8	104.16	100 MHz	F-OFDM	5G FR1
7680	120	9.6	52.08	200 MHz	FF-OFDM	FR1/FR2
7680	240	19.2	26.04	400 MHz	FF-OFDM	FR2/FR2-2
7680	480	38.4	13.20	400 MHz	FF-OFDM	FR2-2/A
7680	960	76.8	6.60	400 MHz	AI-enabled	FR-A/6G

From the results obtained in Tables 4 and 5, the orthogonality and clock synchronization of 3GPP sampling method over Nyquist method are plotted. The experimental results demonstrate a critical divergence between alias-free waveform reconstruction and orthogonality preservation in multi-carrier frameworks. The data indicates that satisfying the Nyquist criterion alone is insufficient for modern OFDM systems. While a Nyquist compliance rate prevents spectral aliasing, it treats the composite signal as a single continuous waveform. It fails to account for the internal, highly sensitive phase and timing relationships required to separate thousands of overlapping orthogonal subcarriers. As shown in the simulations baseline, when the sampling rate is decoupled from subcarrier architecture, the subcarriers bleed into one another, destroying orthogonality and causing catastrophic system degradation. The 3GPP framework mitigates these aberrations by systematic enforcement of a deterministic relationship using a strict mathematical derivative of SCS and FFT size. By directly linking the sampling rate to a power-of-two FFT matrix, the 3GPP technique yields highly specific, quantized sampling intervals. The result obtained in Fig. 6 shows that at 960 GI, the 3GPP method perfectly aligns by obtaining a 960 kHz tone-space, while the Nyquist misaligns with an increased overhead of 993.6 kHz due to the arbitrary clock grid. This has again displayed the supremacy of 3GPP sampling over the Nyquist method in



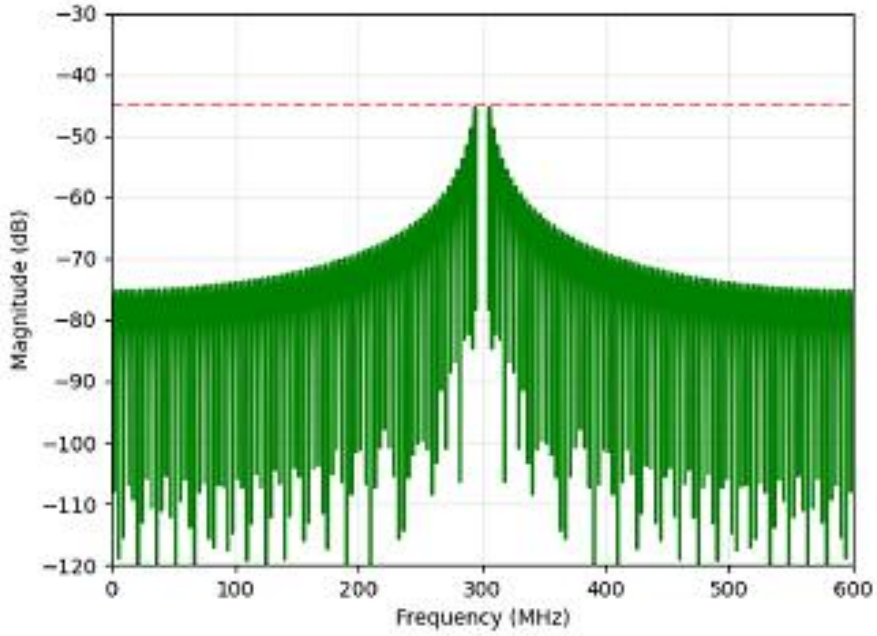
(a) Standard Nyquist Sampling Arbitrary Clock Grid at $f_s = 2 \times B$



(b) 3GPP Sampling Remedy at $f_s = SCS \times N_{FFT}$

Fig. 6 Mitigation of Orthogonality and Clock Synchronization Constraints of Nyquist Sampling by 3GPP Method.

In the course of computing these research results, something phenomenal and fundamental is noticed: the discrepancy between the Nyquist sampling rate and the 3GPP sampling standard based on quadrature modulation becomes glaring. The 3GPP sampling standard is seen to be obtained at 3/4 = 0.75 (that is, $f_S = \frac{4}{3}$BW) of the transmission bandwidth, while the conventional Nyquist sampling rate is derived at $\frac{2}{4} = 0.5$ (that is, $f_S = 2$BW). This conforms to the 3GPP standard demonstrated by equations (2) and (3) and summarized in Table 4. This is noticed in the non-uniformity of the waveform. The 3GPP-recommended sampling rate for QAM is the minimum sampling rate required for any 5G air interface. Fig. 7 clearly illustrates this discrepancy, with -45 dB obtained, which is also the final construction and expectation for the new multi-rate channel access waveform.



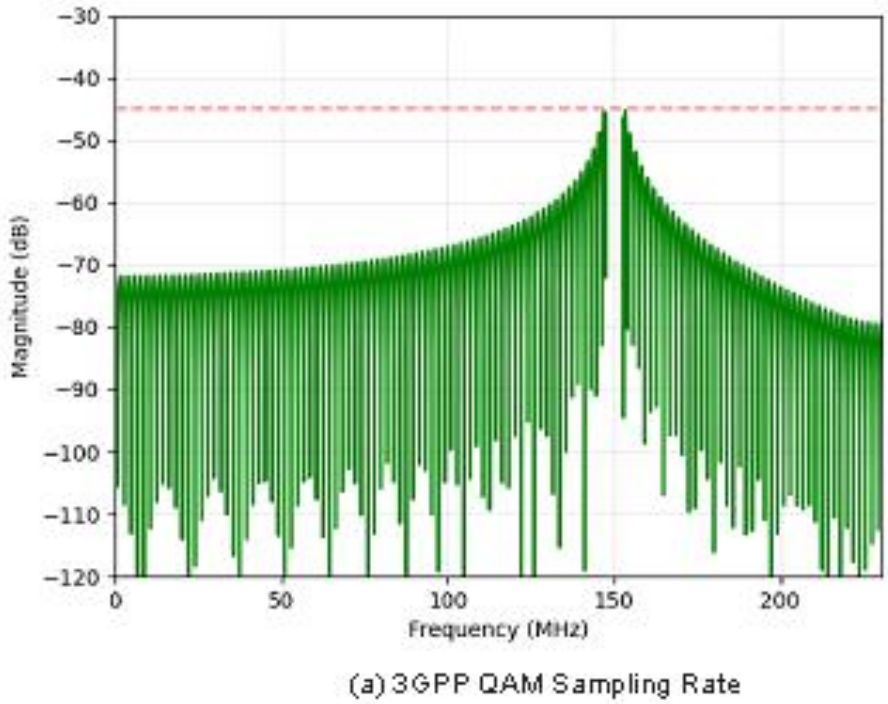


Fig. 7 Nyquist vs. 3GPP QAM Sampling Waveforms within 960 kHz Tone Space

Figures 8 and 9 present the bar chart comparison of the conventional Nyquist sampling model, which could only utilize 50% of its transmission bandwidth to effectively convert analog data into digital, while the 3GPP achieves 75% of its bandwidth. Fig. 9 has also demonstrates this comparison on varying air-interfaces, where it is also glaring that the 3GPP model outperformed the Nyquist in all trials. This simply means that the 3GPP optimizes bandwidth utilization, a requirement for modern and future wireless systems.

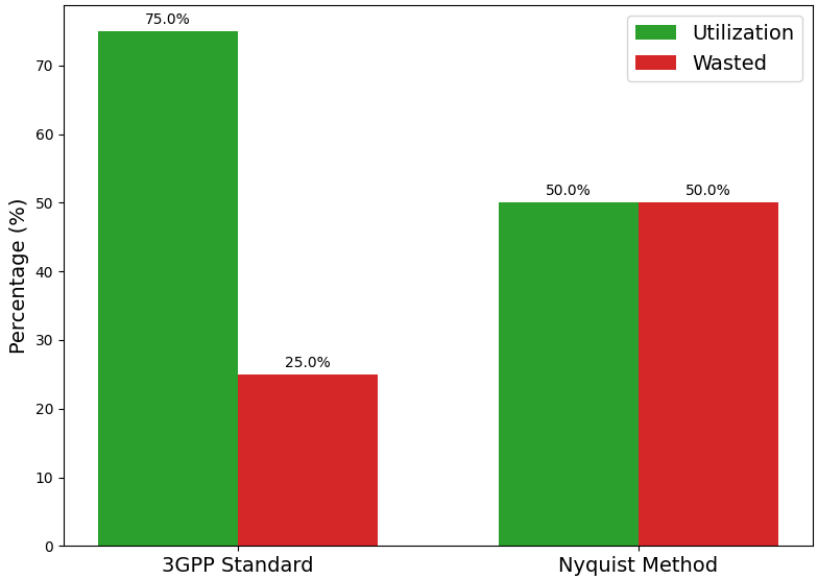


Fig. 8 Bandwidth Utilization versus Waste: 3GPP versus Nyquist

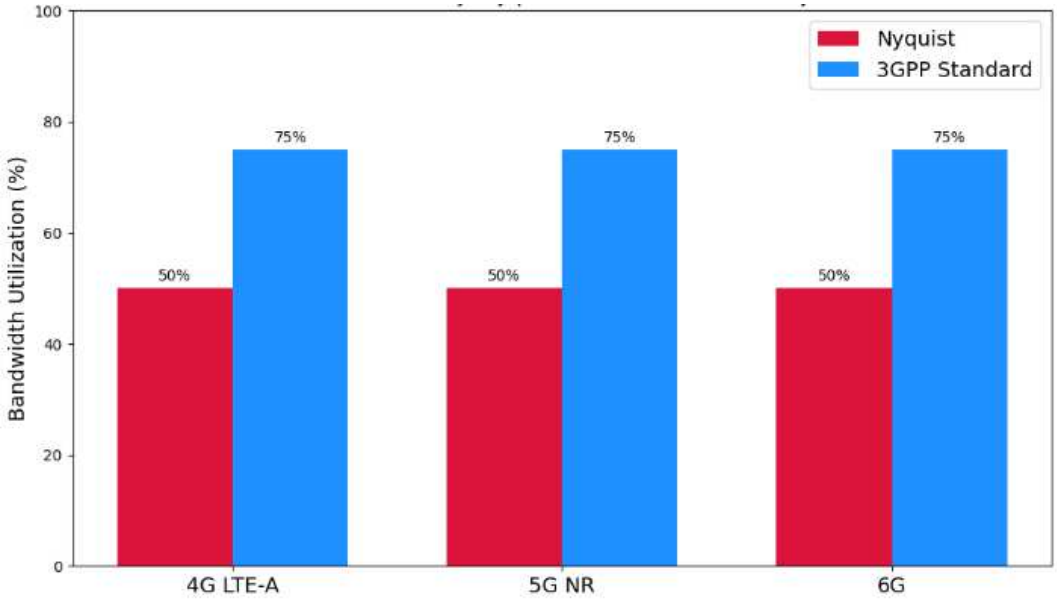


Fig. 9 Bandwidth Efficiency: 3GPP versus Nyquist in Wireless Systems

In summary, the 3GPP wireless sampling standard achieves a better bandwidth utilization of 75.0% (leaving 25.0% waste) compared to the conventional Nyquist method at 50.0% utilization (50.0% waste), establishing it as the preferred approach for 5G NR and 6G architectures. Operating with a signal bandwidth of 20.0 kHz and an RF maximum frequency of 110.0 kHz, the I/Q-based 3GPP framework cuts the per-ADC sampling rate down to 20.0 kHz an 11.0 times (11,0x) reduction relative to the 220.0 kHz Nyquist baseline. This dramatic clock-rate reduction directly translates into tangible hardware benefits, including lower power consumption, higher bit-resolution, and reduced implementation costs.

Conclusion and Further Work

In conclusion, this research presented a comparative analysis between Nyquist and 3GPP sampling techniques. This is aimed at meeting the demand for effective bandwidth utilization in higher wireless communication frequencies. The results show that Nyquist exhibited system efficacy when operated at

half of the transmission bandwidth, which amounts to 50% bandwidth wasted. In contrast, the 3GPP model proved better in bandwidth utilization and spectrum efficiency by maximizing transmission at 75% while wasting only 25%. This 3GPP attainment has aligned with the requirements of modern and next-generation wireless communication systems in terms of increasing bandwidth demand to improve system throughput. In summary, the Nyquist rate provides the bare minimum mathematical sampling rate, while the 3GPP sampling rate is an oversampled-standardized frequency optimized for the digital processing of modern cellular radio waves.

To further advance on this, this research suggests the development of a hybrid sub-Nyquist/compressed sensing (CS) inside 3GPP frames. This novelty integrates CS directly into the baseband Resource Block Groups (RBGs) of 3GPP-compliant frames. This method is expected to solve the problem of high sampling overhead by eliminating the need to process or transmit wideband baseband signals at full Nyquist rates.

Acknowledgment

The authors are deeply grateful to the administration of the Federal University of Applied Sciences, Kachia, Nigeria, for providing the facilities and support necessary to complete this review. Their generosity and encouragement greatly enhanced the quality of this manuscript.

Declaration of competing interest

The authors declare that they have no known competing financial interests or personal relationships that could have appeared to influence the work reported in this paper.

Data availability

Data will be made available on request.

References

1. Ken, P. C. (McGraw-Hill Education) (2011). A comprehensive reference for digital audio engineering, explaining the technical principles behind pulse-code modulation (PCM), quantization, bit depth, and the characteristics of various digital audio file formats. https://apxml.com/courses/applied-speech-recognition
2. Kehtarnavaz, N., Parris, S., & Sehgal, A. (2022). Analog-to-Digital Signal Conversion. In: Smartphone-Based Real-Time Digital Signal Processing, *Synthesis Lectures on Signal Processing. Springer, Cham.* https://doi.org/10.1007/978-3-031-02540-2_4
3. Yao, Y., Sun, J., Miao, P., Chen, G., & Tafazolli, R. (2026). Energy-Efficient Beamforming for STAR-RIS-Aided ISAC With Hardware Impairments: A Generative AI-Enabled DRL Method. *IEEE Transactions on Wireless Communications*. https://doi.org/10.1109/TWC.2026.3692600
4. Wang, Y., Wang, Q., Zheng, X., Song, L., & Ma, X. (2026). Gaussian-Elimination-Free Ordered Statistics Decoding via Pre-Stored Systematic Matrices. *IEEE Transactions on Communications*. https://doi.org/10.1109/TCOMM.2026.3712543
5. Zhang, Y., Zhu, N., Meng, F., Wang, K., Ma, K., & Yeo, K. S. (2026). A 6–10.1-GHz Compact CMOS SOI Power Amplifier Using a 6: 1 Dual-Mode-Optimized Interleaved Transformer for Portable Radar and ISAC Front Ends. *IEEE Journal of Solid-State Circuits*. https://doi.org/10.1109/JSSC.2026.3719376
6. Liu, X., Zhang, H., Li, H., & Sun, C. (2025). Intelligent Beamforming Design for Integrated Sensing, Communication, and Computation. *IEEE Transactions on Communications*, *74*, 1192-1206. https://doi.org/10.1109/TCOMM.2025.3634267
7. Wang, F., Yang, H., Zhang, S., He, X., Zhu, L., & Quek, T. Q. (2026). GEMS: GAT-embedded mobility for dual connectivity in integrated terrestrial and non-terrestrial networks. *IEEE Transactions on Mobile Computing*. https://doi.org/10.1109/TMC.2026.3681814
8. Gade, S. M., Sumana, S. G., Aarthi, S., Ravikumar, R. N., & Swetha, C. B. (2025). Advancing towards 6G Innovations, Challenges and Future Prospects. *6G Impacts on Natural Habitats and Human Life*, 1-26. https://doi.org/10.4018/979-8-3373-2220-9.ch001
9. Siddiky, A. N. M., Rahman, E. M., Uzzal, S. M., & Kabir, D. M. H. (2025). A Comprehensive Exploration of 6G Wireless Communication Technologies, *Computers 2025,* vol. 14, p. 15, 2025. https://doi.org/10.3390/computers14010015
10. Liu, Y., Zhang, F., Zhang, Y., Zhang, S., He, B., Wang, J., & Du, X. (2026). ComStar: Compression-aware stream query for heterogeneous hybrid architecture. *IEEE Transactions on Parallel and Distributed Systems*. https://doi.org/10.1109/TPDS.2026.3662253

11. Zhang, G., & Zhou, S. (2025). A methodology for designing high-efficiency power amplifiers using simple microstrip harmonic tuning circuits. *Electronics*, *14*(23), 4767. https://doi.org/10.3390/electronics14234767
12. Qi, N., Jiang, H., Xiao, S., Wu, D., Zhou, F., Li, C., & Jin, S. (2026). Robust and Energy-efficient Multi-UAV Trajectory Planning for Data Collection: A Game-theoretic and Deep Reinforcement Learning Approach. *IEEE Transactions on Green Communications and Networking*. https://doi.org/10.1109/TGCN.2026.3695901
13. Liao, X., Zhang, Q., Sun, B., & Zheng, X. (2025). Weather forecast-enabled tropospheric scattering path loss modeling for over-the-horizon maritime communications. *IEEE Transactions on Antennas and Propagation*. https://doi.org/10.1109/TAP.2025.3637508
14. Liu, L., Wang, F., Yin, X., Xu, M., Yang, Y., Yu, N., ... & Li, Y. (2025). Low-loss flexible filter based on compact double interdigital coupling SIR with TPV technology for bendable wireless communications. *IEEE Microwave and Wireless Technology Letters*. https://doi.org/10.1109/LMWT.2025.3637823
15. Manganaro, G. (2022). An introduction to high sample rate Nyquist analog-to-digital converters. *IEEE Open Journal of the Solid-State Circuits Society*, *2*, 82-102. https://doi.org/10.1109/OJSSCS.2022.3212028
16. Augustine, Z., Abdu-Aguye, U. F., Yaro, A. S., Bello, H., Tekanyi, A. M. S., Umeonwuka, O. O., ... & Almustapha, M. D. (2025). Wireless multi-carrier transmission techniques for commercial deployment in LTE, LTE-A, and 5G FR1. *Journal of Electrical Systems and Information Technology*, *12*(1), 77. https://doi.org/10.1186/s43067-025-00270-5
17. Höyhtyä, M., Apilo, O., & Lasanen, M. (2018). Review of latest advances in 3GPP standardization: D2D communication in 5G systems and its energy consumption models. *Future Internet*, *10*(1), 3. https://doi.org/10.3390/fi10010003
18. Lin, X. (2025, May). 3GPP evolution from 5G to 6G: A 10-year retrospective. In *Telecom* (Vol. 6, No. 2, p. 32). MDPI. https://doi.org/10.3390/telecom6020032
19. Giuliano, R. (2024). From 5G-advanced to 6G in 2030: New services, 3GPP advances, and enabling technologies. *IEEE Access*, *12*, 63238-63270. https://doi.org/10.1109/ACCESS.2024.3396361
20. He, X., Yang, Z., Li, D., Zeng, J., Jiang, T., & Chen, S. (2026). Dual-Stage Reinforcement Learning-Based Beam Tracking for Integrated Sensing and Communications in V2I Scenarios. *IEEE Transactions on Wireless Communications*. https://doi.org/10.1109/TWC.2026.3654423
21. Stoynov, V., Poulkov, V., Valkova-Jarvis, Z., Iliev, G., & Koleva, P. (2022). Ultra-dense networks: Taxonomy and key performance indicators. *Symmetry*, *15*(1), 2. https://doi.org/10.3390/sym15010002
22. Achimugu, P., Augustine, Z., Jubrin, A. A., Lanihun, O., Yoro, E. R., Abba, A. A., and Hamisu, A. (2025). A Survey of Wireless Cellular Network Generations and Their Channel Access Techniques. *Journal of Computing and Social Informatics*, vol. *5*, no. 1, pp. 1–12, 2025. https://doi.org/10.33736/jcsi.8835.2026
23. Tera, S. P., Chinthaginjala, R., Pau, G., & Kim, T. H. (2024). Toward 6G: An overview of the next generation of intelligent network connectivity. *IEEE Access*, *13*, 925-961. https://doi.org/10.1109/ACCESS.2024.3523327
24. Augustine, Z., Bello, H., Tekanyi, A. M., Yaro, A. S., Abdulkareem, H. A., Umeonwuka, O. O., & Abdu-Aguye, U. F. (2025). Generation of 5G frequency one model based on orthogonal multiple access technique of filtered-orthogonal frequency division multiplexing scheme for advanced interference evaluation. *Computers and Electrical Engineering*, *123*, 110056.. https://doi.org/10.1016/j.compeleceng.2024.110056
25. Sun, J., & Zhou, S. (2025). Cuckoo search-ExtraTrees model for Radio-frequency power amplifier under different temperatures. *Frequenz*, *79*(7-8), 433-438. https://doi.org/10.1515/freq-2024-0298
26. Di, B., Zhang, Y., Deng, R., Wang, M., Sun, S., & Song, L. (2025). Holographic metasurfaces for extremely large-scale MIMO communications: Design, implementation, and experiment results. *IEEE Wireless Communications*. https://doi.org/10.1109/MWC.2025.3625029
27. Li, Y., Geng, H., Tong, W., Xiao, H., Liu, Y., & Meng, Y. (2026). Reliability Assessment of Communication Systems Via Host–Guest Generative Cooperative Modeling in Antenna-Port Electromagnetic Environments. *IEEE Transactions on Reliability*. https://doi.org/10.1109/TR.2026.3722853
28. Wang, X., Chen, Q., Jia, M., & Gu, X. (2022). Wideband spectrum sensing based on advanced sub-Nyquist sampling structure. *EURASIP Journal on Advances in Signal Processing*, *2022*(1), 41. https://doi.org/10.1186/s13634-022-00874-3
29. Ou, Z., Liu, X., & Yang, H. (2022). A low sampling rate receiver design for multi-antenna multi-user OFDM systems. *Entropy*, *24*(4), 448. https://doi.org/10.3390/e24040448
30. Liu, S., Zhang, C., Zhang, J., Liu, X., Zhu, B., & Tian, C. (2024). Sub-Nyquist sampling-based high-frequency photoacoustic computed tomography. *Optics Letters*, *49*(7), 1648-1651. https://doi.org/10.1364/OL.515650
31. Khan, Z. U., O'Farrell, T., & Ford, K. L. (2023, September). Direct IF sampling receivers for 5G millimeter-wave communications systems. In *2023 IEEE 34th Annual International Symposium on Personal, Indoor and Mobile Radio Communications (PIMRC)* (pp. 1-5). IEEE.

32. Zheng, W., Li, D., Wang, R., Chen, M., Zhang, Z., & Ge, R. (2025). Sub-Nyquist sampling rate temporal correlation method for measuring the surface of the transparent planar element. *Optics Express*, *33*(6), 13316-13331. https://doi.org/10.1364/OE.551309
33. Mello, M., Silva, D., & Mendes, L. (2026). A multiple access approach for faster-than-Nyquist GFDM systems. *Wireless Networks*, *32*(2), 797-814. https://doi.org/10.21203/rs.3.rs-6113599/v1
34. Dong, X., Zhao, J., Zhou, Z., Chen, P., Zhang, H., & Dang, X. (2025). DOA estimation of non-circular signals with nested arrays: a block tensor sparse representation. *IEEE Transactions on Aerospace and Electronic Systems*. https://doi.org/10.1109/TAES.2025.3647621
35. Liu, X., Chen, C., & Fischione, C. (2025). Cell-free ISAC systems: Learning-based channel estimation and coordinated beamforming. *IEEE Transactions on Cognitive Communications and Networking*. https://doi.org/10.1109/TCCN.2025.3633745
36. Taskiran, S. F., Turkoglu, B., Kaya, E., & Asuroglu, T. (2025). A comprehensive evaluation of oversampling techniques for enhancing text classification performance. *Scientific Reports*, *15*(1), 21631.. https://doi.org/10.1038/s41598-025-05791-7
37. Yousefimehr, B., Ghatee, M., Fazli, J., Ghaffari, S., Rafei, Z., Seifi, M. A., ... & Mousavi, N. S. (2026). Data Balancing Strategies: A Systematic Survey of Resampling and Augmentation Methods. *Machine Learning and Knowledge Extraction*, *8*(7), 211. https://doi.org/10.3390/make8070211
38. Marathe, K. C. (2021). Sampling Rate in LTE and 5G NR Baseband Systems, *IEEE Communication Society Bangalore India Newslette*r, vol. 9
39. Teamques10, 2020. https://www.ques10.com/p/48274/orthogonal-frequency-division-multiple-access-ofdm/
40. 3GPP TS 36.101, V17.6.0. (2022). Physical Layer for Sampling Frequency. LTE; Evolved Universal Terrestrial Radio Access (E-UTRA); User Equipment (UE) Radio Transmission and Reception. 2022. *https://www.etsi.org/deliver/etsi_ts/136100_136199/136101/17.06.00_60/ts_136101v170600p.pdf*
41. Iadarola, G., Daponte, P., De Vito, L., & Rapuano, S. (2023). Over the limits of traditional sampling: Advantages and issues of AICs for measurement instrumentation. *Sensors*, *23*(2), 861. https://doi.org/10.3390/s23020861
42. Augustine, Z., Yaro, A. S., Maly, F., Pavel, P., Umeonwuka, O. O., & Sambo, P. B. (2025, November). The Effectiveness of Cyclic Prefix Technique in 5G and 6G Wireless Networks Relative to its Subcarrier Spacing and Processing Time. In *2025 IEEE Connecting the Unconnected Europe, Middle East, and Africa Regional Summit (CTUS-EMEA)* (pp. 1-6). IEEE. https://doi.org/10.1109/CTUS-EMEA68989.2025.11592242